Physicochem. Probl. Miner. Process., 54(2), 2018, 311-320

http://www.journalssystem.com/ppmp

Physicochemical Problems of Mineral Processing

ISSN 1643-1049

Received February 26, 2017; reviewed; accepted July 08, 2017

Interaction between sphalerite and pyrite and its effect on surface oxidation of sphalerite

Bo Yang, Xian Xie, Xiong Tong, Zhuoyue Lan, Yiqi Cui

Kunming University of Science and Technology, Faculty of Land Resource Engineering, Kunming 650093, China

Corresponding author: xiongtong2000@yahoo.com (Xiong Tong)

Abstract: The interaction between sphalerite and pyrite was investigated by dissolution test, X-ray photoelectron spectroscopy (XPS), zeta potential measurement and density functional theory (DFT) calculation. Dissolution tests indicated that sphalerite dissolution was promoted due to the galvanic interaction between sphalerite and pyrite. The Zn^{2+} ion concentration increased with increasing pyrite content and dissolved time. XPS analysis results demonstrated that a new oxidation product was formed on the sphalerite surface in the presence of pyrite in a pulp. Zeta potential measurements showed that the isoelectric point of sphalerite increased from 3.3 to 5.4 due to galvanic interaction. DFT calculation results suggested that electron transfer from sphalerite to pyrite occurred when they contacted. The Zn 4s and S 3p states of sphalerite lost electrons. The Fe 4p and 4s of pyrite states obtained electrons, and Fe 3d and S 3s states lost a small number of electrons. The surface oxidation of sphalerite was promoted due to the interaction with pyrite, and the collectorless floatability of sphalerite decreased.

Keywords: *sphalerite, surface oxidation, minerals interaction, DFT*

1. Introduction

Sphalerite is an important zinc resource for zinc metal production. The selective separation of sphalerite from its associated sulfide minerals is usually carried out by froth flotation (Celik, 2015; Ejtemaei and Nguyen, 2017; Mikhlin et al., 2016a). Pyrite, as a common gangue mineral, is usually associated with sphalerite (Mu et al., 2016; Zhang et al., 1997). In the selective flotation of sphalerite, a large amount of lime is used to depress pyrite. However, the flotation practices in several processing plants indicated that the recovery and grade of zinc concentrates were affected by the proportion and reactivity of pyrite in ores. The selective separation of sphalerite from pyrite is remarkably difficult due to the competitive adsorption of sphalerite and pyrite for activator (e.g. copper sulfate) and collector (e.g. xanthate). The presence of pyrite in Zn concentrates also has a detrimental effect on the grade of concentrates (Gerson et al., 1999; Owusu et al., 2014).

Many studies have suggested that the high pyrite content in ores will result in a difficulty in selective separation of valuable minerals from pyrite and a high reagent consumption (Qingyou et al., 2007; Trahar et al., 1994; Urbano et al., 2007). However, except for the finely disseminated ores, the interactions between mineral/mineral and mineral/grinding medium are also an important factor affecting the selective separation. In the presence of those interactions, the floatability of the mineral with a higher rest potential is enhanced, while that with a lower rest potential is decreased (Ekmekçi and Demirel, 1997). Qin et al. (2015) suggested that pyrite did not change the oxidative and reductive products of galena surface, but it increased the current density and oxidation rate during galena oxidation. Consequently, the floatability of galena and pyrite decreased and increased, respectively. Owusu et al. (2015) studied the interaction between chalcopyrite and pyrite and found that chalcopyrite exhibited poor flotation performance under different aeration conditions. The amount of air required to achieve a good chalcopyrite flotation was correlated positively with the mass fraction

http://dx.doi.org/10.5277/ppmp1816

of pyrite in the pulps. Furthermore, the pyrite in chalcopyrite/pyrite mixtures was activated by Cu^{2+} ions dissolved from chalcopyrite surface, and floatability was enhanced.

Sphalerite, the most important and abundant zinc sulfide mineral, is commonly associated with pyrite. The fundamental aspects of sphalerite flotation have been studied thoroughly, and the related mechanisms containing copper activation and reaction with a thiol collector were explained and understood (Chandra and Gerson, 2009). The difficulty in the selective separation of sphalerite from associated pyrite is mainly regarded as the accidental activation of pyrite and competitive adsorption for Cu^{2+} ion and xanthate. However, the interaction between sphalerite and pyrite and its effect on surface characteristics have not been studied thoroughly due to the special properties of sphalerite, which needs to be activated prior flotation and has a higher band energy of 3.7 eV than other sulfide minerals (Liu et al., 2013). In addition, it has been demonstrated that the rest potential for the common sulfide minerals are classified in an increasing order as follows: ZnS < PbS < $CuFeS_2$ < FeS_2 (Santos et al., 2016). From the viewpoint of electrochemistry, the difference in the rest potential is an important driving force that promotes the transfer of electrons between minerals. According to this order, a large difference in the rest potential was observed between sphalerite and pyrite, but the study about the interaction between sphalerite and pyrite has been rarely reported. In this paper, the interaction between sphalerite and pyrite was studied by using the dissolution test, X-ray photoelectron spectroscopy (XPS) surface analysis and zeta potential measurement. The density functional theory (DFT) method was used to obtain further details about the interaction, and the issues could be further and better explained by this study.

2. Experiment

2.1 Minerals

The highly-mineralized sphalerite and pyrite samples used in this study were obtained from Yiliang Chihong Mine, Yunnan Province, China. After the manual removal of gangue minerals, such as quartz and calcite, the samples were dry-ground in a porcelain ball mill and dry-screened using nylon sieves to obtain the desired particle size. The sample was prepared only prior to its use to prevent the surface oxidation. The chemical compositions of sphalerite and pyrite samples are listed in Table 1. The X-ray diffraction analysis results showed that the samples used in this study were of high purity.

Table 1. Chemical compositions of sphalerite and pyrite samples (%). Dissolution tests

Elements	Zn	Fe	S	Pb	SiO_2
Sphalerite	63.26	1.04	33.25	0.43	0.93
Pyrite	0.006	53.26	46.16	0.21	0.22

Analytical-grade HCl and NaOH from Tianjin No. 3 Chemical Reagent Factory, and ultrapure water with resistivity of 18.25 $M\Omega/cm^{-1}$ were used. Sphalerite and pyrite with -0.074/+0.048 mm particles size were used in dissolution tests.

Sphalerite or mixture of pyrite and sphalerite was added in a 100 cm^3 reaction vessel with the 50 cm^3 ultrapure water. The temperature of suspension was kept constant at 25 °C by a thermostatically controlled water bath, and the pH of suspension were adjusted by HCl and NaOH solutions. A magnetic stirrer was used for the stirring of the suspension at a speed of 600 rpm. After dissolution with the given time intervals, the suspension was separated by using a centrifuge at 3500 rpm for 10 min. After acidification, the aqueous solution was subjected to the Zn^{2+} concentration analysis by using ICP-MS (7700X, Agilent, USA).

2.2 XPS surface analysis

The samples used for XPS study were prepared by the following procedure. The sphalerite block with 0.6×0.6×0.2 cm size was wet-polished with 1200 grit polishing paper for 2 min. Then, the sample was washed with ultrapure water and immersed quickly in the suspension containing the 1.0 g pyrite of -0.048 mm. The sphalerite surface subjected to XPS measurement was exposed to the suspension, and the pH value of suspension was controlled by HCl and NaOH solutions. Mechanical agitation was

used for the stirring of the suspension. After stirring for 20 min, the sphalerite block was taken and washed with ultrapure water and dried at vacuum environment. The solution containing pyrite particles was filtrated and washed with ultrapure water, and the solid samples was dried at vacuum environment. After that, XPS measurements were carried out using a PHI5000 Versa ProbeII (PHI5000 ULVAC-PHI, Japan) equipped with a monochromatic Al Kα X-ray source at 1486.6 eV. The pressure of the analyzer chamber was 10^{-8} Pa during analysis. The analyzed samples were first subjected to a survey scan to identify the chemical components and subsequent high-resolution scans on a certain element. The spectra and surface atomic concentration were obtained and calculated based on the MultiPak Spectrum software.

2.3 Zeta potential measurements

In zeta potential measurements, sphalerite and pyrite with different particle sizes were used in order to separate prior tests by settling. Before measurements, the pyrite with −0.063+0.038 mm particles size was subjected to ultrasonic cleaning to remove any adhering fine particle, which might influence the zeta potential of sphalerite. After cleaning, the sphalerite with −0.010 mm particles size was mixed with pyrite for 10 min by using magnetic stirring to improve the interaction between sphalerite and pyrite. At the end of stirring, the suspension was settled for a specified time. Subsequently, the supernatant suspension of sphalerite was taken using a syringe for zeta potential measurements. Blank tests showed that a negligible amount of remaining pyrite was present in the analyzed sample. The zeta potential was carried out using the Malvern Zetasizer Nano ZS90.

2.4 DFT study

The interaction between sphalerite and pyrite was investigated by using first-principle calculations with CASTEP and GGA-PW91 based on DFT. Sphalerite with the crystal parameters of a=b=c=5.4301 Å and pyrite with the crystal parameters of a=b=c=5.4209 Å were used in calculation. The relaxed sphalerite (110) and pyrite (110) surfaces using the building layer tools (Gao et al., 2014). The interaction model was established. Only valance electrons were considered by using ultrasoft pseudopotentials. A plane wave cut-off energy of 340 eV and a 3×3×3 Monkhorst-Pack *k*-point sampling grid were used. The self-consistent field convergence tolerance was set to 2.0×10^{-6} eV/atom. All calculation parameters used in geometry optimization and properties calculation were identical.

2.5 Microflotation tests

Flotation tests were conducted in 40 cm^3 flotation cell (Gao et al., 2016; Wang et al., 2016) with 4.0 g of −0.106+0.075 mm sphalerite or pyrite sample for each test. In addition, the total of 4.0 g mineral mixtures with 50% pyrite was used to investigate the effect of pyrite on sphalerite floatability. The sample was first mixed with 40 cm^3 of ultrapure water and conditioned at the specified pH values for 5 min, the frother MIBC with the dosage of 5 mg/dm^3 was added and conditioned for 2 min. Then, the slurry was floated for 4 min. Finally, the floated and non-floated particles were collected and assay for the calculation of recovery. All of tests were repeated three times under the same conditions, the recovery reported in this paper is the average.

3. Results and discussion

3.1 Effects of pyrite on dissolution behavior of sphalerite

In the suspension containing sphalerite and pyrite, the Zn^{2+} ions in solution mainly derive from the surface dissolution of sphalerite. The concentration of Zn^{2+} is an important indicator for the surface oxidation of sphalerite. Due to the flotation of sphalerite was usually conducted at neutral or alkaline pH ranges and pyrite is easy to be oxidized at alkaline pH ranges, which results in a high concentration of Fe^{3+} in pulp. Therefore, a neutral pH was chosen, and Table 2 shows the concentration of Zn^{2+} ions in solution with different pyrite proportions and dissolved times.

In the absence of pyrite, the Zn^{2+} concentration only shows a negligible increase from 0.1099×10^{-6} g/cm^3 to 0.1897×10^{-6} g/cm^3 with the increase of dissolution time from 5 min to 50 min. However, the Zn^{2+} concentration presents a significant increase when the presence of pyrite in the suspension. The Zn^{2+} concentration increases with the increasing pyrite content from 0.1099×10^{-6}

g/cm^3 to 8.048×10^{-6} g/cm^3 at 5 min, and further increases with the increase of dissolved time. Results from Table 2 show that pyrite accelerates the surface dissolution of sphalerite and causes a high Zn^{2+} concentration in solution. It well be known that the surface dissolution of mineral particles is related with the surface oxidation of mineral surfaces. Evidently, the surface oxidation of sphalerite is promoted when the presence of pyrite in pulp. From the hydrometallurgical viewpoint, it has been suggested that pyrite can catalyze the leaching kinetics of sphalerite due to the galvanic interaction between them (Estrada-de los Santos et al., 2016).

The surface oxidation of sphalerite exerts two influences on flotation. First, a mild oxidization status is beneficial for the formation of hydrophobic species, such as elemental sulfur and metal-deficient polysulfide on sphalerite surface, which improves the collectorless floatability of sphalerite. Second, an excessive oxidization status is detrimental for flotation due to the formation and adsorption of hydrophilic hydroxyl complex on sphalerite surface, which reduces the floatability of sphalerite and the adsorption of collectors and activators (Chen et al., 2014; Cruz et al., 2005; Urbano et al., 2007).

Table 2. Zn^{2+} ion concentrations in the absence and presence of pyrite (pH=7.3)

Dissolved time	$C_{Zn^{2+}}$ (10^{-6} g/cm^3)		
(min)	2.0 g ZnS	2.0 g ZnS+1.0 g FeS_2	2.0 g ZnS+2.0 g FeS_2
5	0.1099	5.7572	8.0480
10	0.1202	6.7873	10.4603
20	0.1359	6.7931	10.9890
30	0.1879	7.1908	11.9814
50	0.1897	8.7378	13.2283

3.2 XPS study

XPS was employed to further study the surface differences and oxidation products of sphalerite before and after interaction at pH=7.3. Fig. 1 shows the Zn 2p and S 2p spectra of sphalerite alone and contacting with pyrite. Accordingly, the Fe 2p and S 2p spectra of pyrite surface are also displayed in Fig. 1.

Fig. 1 shows that the Zn 2p spectra are composed of a strong peak Zn $2p_{3/2}$ at binding energy of 1022.0 eV and a Zn $2p_{1/2}$ at binding energy of 1045.0 eV. The Zn 2p spectra from the sphalerite alone and contacting with pyrite remains almost unchanged, which indicated that the interaction between sphalerite and pyrite exerts no influence on the chemical status of Zn atom on ZnS surface. However, when pyrite is present in the pulp, the S 2p spectra on sphalerite surface show a change on peak shape and peak areas. This result indicated that the chemical status of S atom on sphalerite surface is altered due to the presence of pyrite in pulp. Similar changes can be detected in Fe 2p and S 2p spectra of pyrite surface, only the chemical status of S atom on pyrite surface was observed after contacting with sphalerite.

Fig. 2 shows the changes of S 2p on sphalerite and pyrite surface before and after interaction. Many studies have suggested that S 2p spectra are fitted using the S $2p_{1/2}$ and S $2p_{3/2}$ doublet with a fixed 1:2 peak area ratio and 1.18 eV energy separation (Chen et al., 2014; Harmer et al., 2008; Mu et al., 2017). On the sphalerite surface, the S2p doublet with the S$2p_{3/2}$ at binding energy of 161.24 eV is attributed to S^{2-} from sphalerite surface or bulk. The broad peak with the S $2p_{3/2}$ at binding energy of 162.07 eV represents the S_2^{2-} formed during surface oxidation. However, a new peak with the S $2p_{3/2}$ at binding energy of 163.09eV occurs at the S 2p spectra of sphalerite after contacting with pyrite, this peak is associated with the formation of S_n^{2-} or S^0 on sphalerite surface (Ejtemaei et al., 2016).

On the pyrite surface, the doublet with the S $2p_{3/2}$ at binding energy of 162.64 eV is attributed to the S_2^{2-} from pyrite surface and bulk (Mu et al., 2016). After contacting with sphalerite, a broad peak with the S $2p_{3/2}$ at binding energy of 160.74 eV can be detected on pyrite surface, which is identified as the S^{2-} formed on the pyrite surface (Fornasiero et al., 1994).

Results from Figs. 1 and 2 indicated that the interaction between sphalerite and pyrite in pulp has a significant effect on the surface oxidation characteristics of sphalerite. The surface oxidation of

sphalerite is promoted due to galvanic interaction, which results in the formation of S_n^{2-} or S^0 on sphalerite surface.

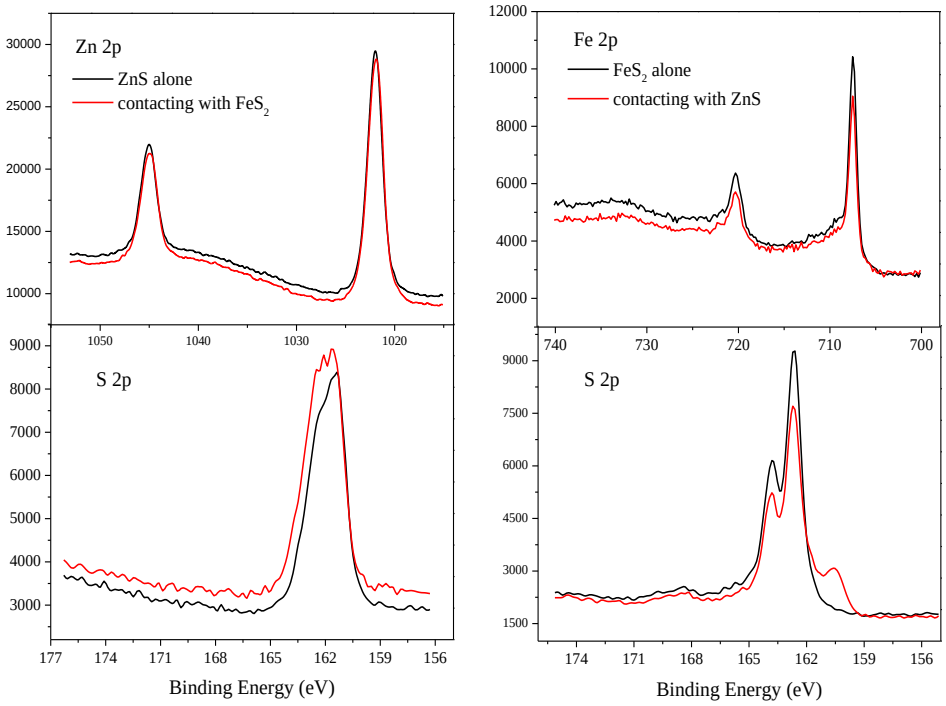

Fig. 1. Zn 2p, Fe 2p, and S 2p spectra for ZnS and FeS_2 surfaces

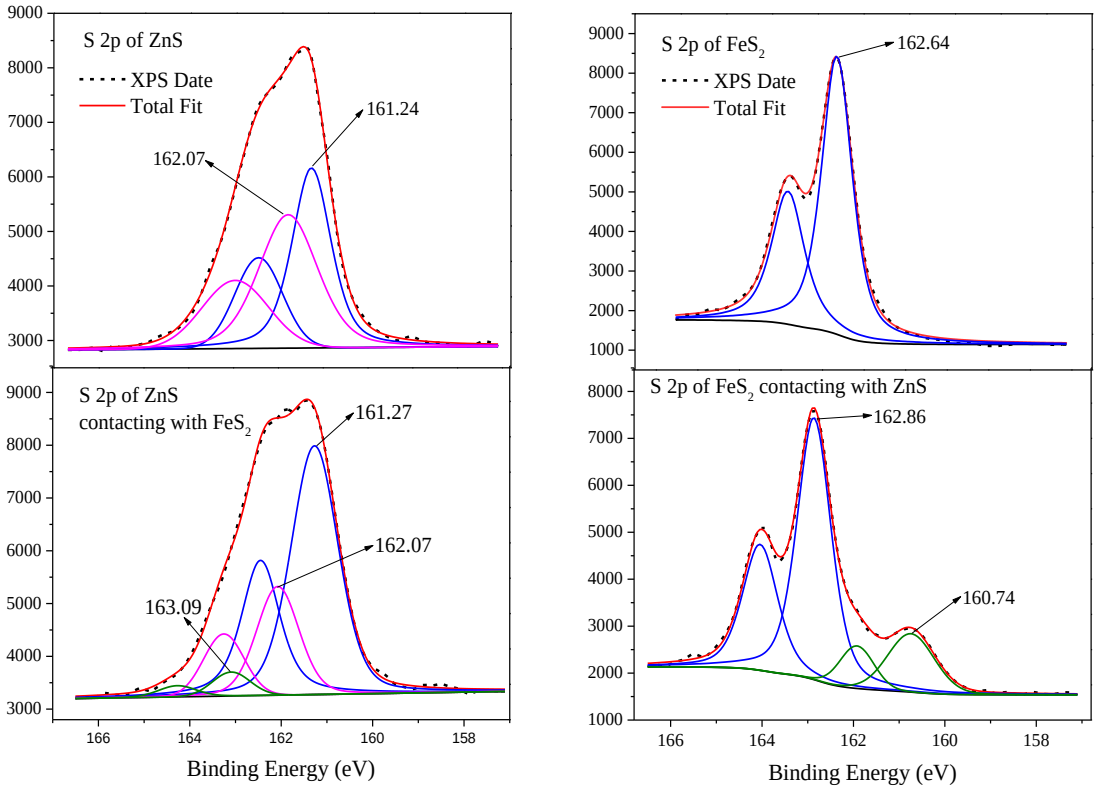

Fig. 2. S2p spectra of ZnS and FeS_2 alone and mixtures

3.3 Zeta potential

It has been demonstrated that the surface oxidation of minerals can enhance its isoelectric point due to the adsorption of metal ions or hydroxy complexes on minerals surface, the unoxidized sphalerite surface has an isoelectric point at around pH=3.0 (Nooshabadi and Rao, 2014; Leiro et al., 2017). In the present study, the effect of the interaction between sphalerite and pyrite on the isoelectric point of sphalerite was measured, and the results are shown in Fig. 3. For sphalerite and pyrite, the zeta potential steadily decreases with increasing pH. The isoelectric point of sphalerite and pyrite are approximately 3.3 and 3.1 respectively, which is similar to the values reported by Shaoxian Song and Alejandro Lopez-Valdivieso (Song et al., 2001).

However, the isoelectric point of sphalerite significantly increases from 3.3 to 5.4 when the presence of pyrite in pulp. This increase may be caused by the galvanic interaction between sphalerite and pyrite, which promotes the surface oxidation of sphalerite and the formation of sulfur–oxygen species on surface, as described in the dissolution tests and XPS study. The oxidation products and Zn^{2+} ions can migrate or adsorb on the mineral surface, which increases the zeta potential of sphalerite.

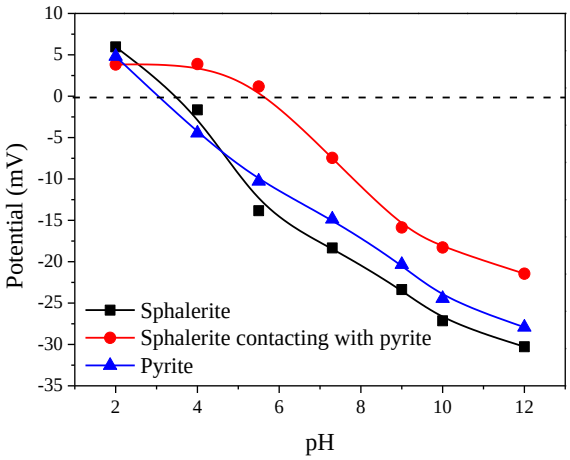

Fig. 3. Zeta potentials of sphalerite alone and sphalerite mixed with pyrite

3.4. DFT calculation

DFT calculation is a useful tool to study the crystal structure of minerals and the interaction, adsorption and reaction of flotation reagents with mineral surfaces (Gao et al., 2017; Hu et al., 2012). The simulation and calculation may be helpful for the explanation of some phenomena that cannot be observed through experimental studies (Feng et al., 2017). In the present study, the electron transfer and surface interaction between sphalerite and pyrite were investigated by DFT methods. The calculation model was established by combining the relaxed sphalerite (110) surface with the relaxed pyrite (110) surface, as shown in Fig. 4. The density of states (DOS) of surface atoms on sphalerite and the electron transfer between sphalerite and pyrite surfaces were also studied.

Fig. 5 shows the Zn 4s, Zn 3p, and Zn 3d states of sphalerite surface changes before and after contacting with pyrite at a distance of 3.752 Å. The Zn 4s and Zn 3d DOSs at 4.0 eV are significantly reduced when in contact with pyrite, which indicated that Zn atoms on sphalerite surface lose a large number of electrons. In addition, the DOSs of Zn atom on sphalerite surface exhibit a slight shift to the direction of valence band due to the contact with pyrite. The similar change can be observed on the S 3s and 3p states on sphalerite surface. The S 3p DOS at approximately 5.0 eV disappears, and the S 3p DOS reduces at the Fermi level. These results indicated that the S atoms on sphalerite surface lose a fraction of electrons, and the electron activity in S 3p orbital weakens due to the galvanic interaction between sphalerite and pyrite (Jiao et al., 2016).

Table 3 shows the electron transfer between sphalerite and pyrite surfaces and the charge number of surface atoms. By surface atomic charge analysis, the electron transfer between mineral surfaces was further studied. For sphalerite surface, Zn 4s and S 3p states lose electrons, and the change in the

number of Zn 4s electrons is higher than that of S 3p electrons. The Zn 3p obtains a small number of electrons, and the Zn 3d and S 3s electron numbers shows no change. Zn 4s state loses many electrons, which increases the positive charge of Zn atom. In addition, S 3p on sphalerite surface loses a small amount of electrons, thereby resulting in oxidation and the decrease in the negative charge of surface S atoms (Long et al., 2016). This oxidation will promote the formation of surface sulfur elements or polysulphide on sphalerite surface, as shown by XPS surface analysis. For pyrite surface, Fe 4s and 4p states obtain electrons, and the change in the number of Fe 4s electrons is considerably less than that of Fe 4p electrons. The Fe 3d state loses a small number of electrons, and the total positive charge number decreases. In addition, S 3p state on pyrite surface loses a small fraction of electrons and the S 3s state electrons number is not changed, but the change in charge number of S atom is negligible (Ke et al., 2016).

Based on the above results, the electron transfer from sphalerite to pyrite will occur when the sphalerite is in contact with pyrite. This electron transfer promotes the oxidation or reduction of mineral surface. Accordingly, the surface oxidation of sphalerite is intensified. A large amount of zinc ions is released from sphalerite surface, and floatability is decreased due to oxidation. However, pyrite surface oxidation is alleviated, and the floatability is enhanced due to its contact with sphalerite (Martin et al., 1989; Mikhlin et al., 2016b).

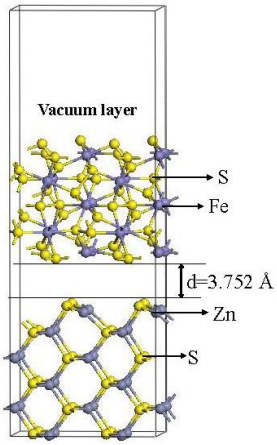

Fig. 4. Computational model used in density functional theory study

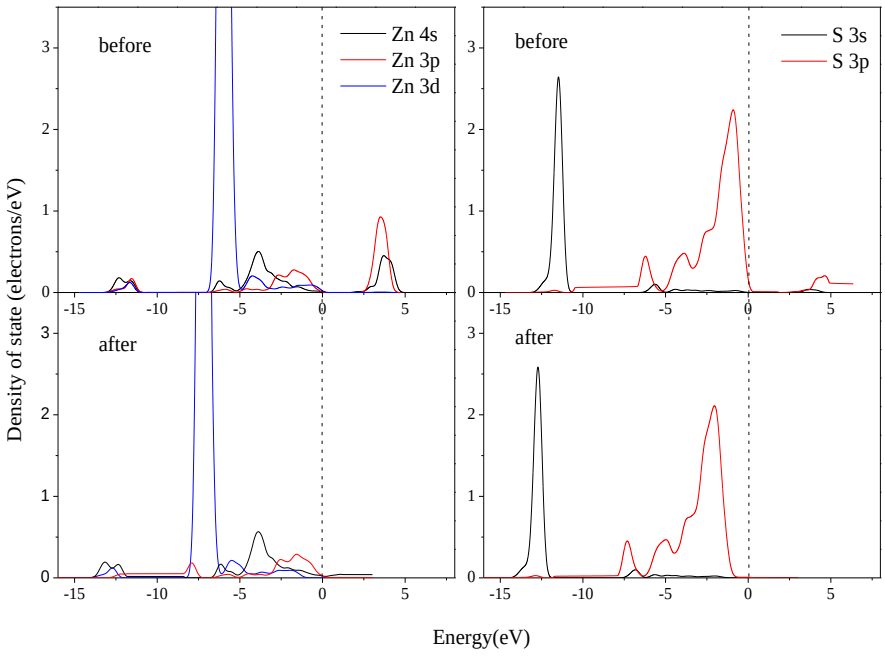

Fig. 5. Density of states of sphalerite surface Zn and S before and after contact

Table 3. Mulliken charge population of atoms on sphalerite and pyrite surfaces

	Atom	Combination	s	p	d	Charge (e)
ZnS	surface Zn	before	0.91	0.76	9.98	+0.36
		after	0.82	0.79	9.98	+0.39
	surface S	before	1.85	4.68	0.00	-0.50
		after	1.85	4.63	0.00	-0.48
FeS_2	surface Fe	before	0.37	0.27	7.14	+0.21
		after	0.39	0.36	7.12	+0.13
	surface S	before	1.82	4.33	0.00	-0.15
		after	1.82	4.31	0.00	-0.14

3.5. Microflotation

Flotation tests were carried out to investigate the influence of interaction on collectorless floatability of sphalerite and pyrite under different pH. The recovery of sphalerite alone and mixing with pyrite as a function of pH are shown in Fig.6.

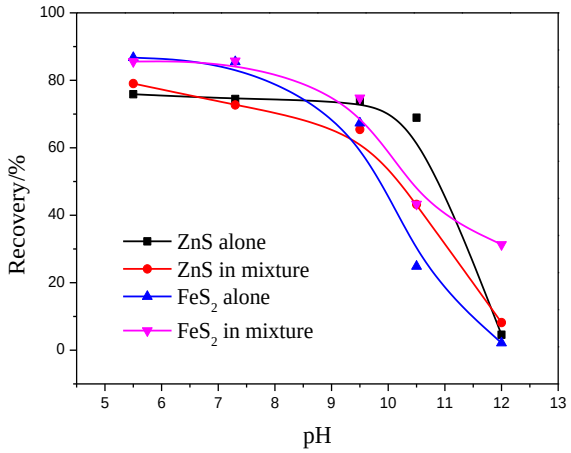

Fig.6. The recovery of sphalerite alone and mixing with pyrite as a function of pH

It is evident from Fig.6 that the flotation behavior of sphalerite and pyrite in mixture was different from the behavior of the individual. The recovery of sphalerite in mixture was decreased at the pH ranges of 7 to 12 compared with single sphalerite. For pyrite, however, the recovery was increased at the pH ranges of 7 to 12 compared with single pyrite.

The decrease in floatability of sphalerite in the presence of pyrite is attributed to the electrochemical interaction between sphalerite and pyrite. Rao and Finch have suggested that the galvanic interaction between a noble minerals and a active minerals will directly affect the floatability of both minerals (Finch and Rao, 1988; Rao and Natarajan, 1989). In the galvanic couple of sphalerite and pyrite, pyrite has the highest electrode potential while the electrode potential of sphalerite is relatively low. When the two minerals contacting each other, the surface oxidation of sphalerite is promoted and pyrite is inhibited, as shown by dissolution tests and XPS analysis. Accordingly, the floatability of sphalerite was decreased while pyrite was increased. The results from flotation tests further confirmed the effect of interaction between sphalerite and pyrite on the surface oxidation of sphalerite, the presence of pyrite in pulp will increase the surface oxidation of sphalerite.

4. Conclusions

The interaction between sphalerite and pyrite will occur when the two minerals contact each other in pulp, and the surface dissolution of sphalerite was enhanced due to galvanic interaction. A new oxidation product on sphalerite surface was detected by XPS analysis. However, the chemical status of S atom on pyrite surface is not changed, except for a metal-deficient S^{2-} formation on pyrite surface.

During the interaction between sphalerite and pyrite, the Zn 3p and S 3p states on sphalerite surface lose most of electrons resulting in the change in charge number of surface Zn and S atoms. For pyrite surface, Fe 4s and 4p states obtain electrons, whereas the S 3p state loses a small fraction of electrons. The electron was transferred from sphalerite to pyrite when sphalerite contacting with pyrite. Accordingly, the surface oxidation of sphalerite was enhanced and the collectorless floatability is decreased, whereas that of pyrite is enhanced.

Acknowledgements

The authors are grateful for the financial support provided by the Applied Basic Research programs of Yunan Province (2014FA027).

References

CHANDRA, A.P., GERSON, A.R., 2009. *A review of the fundamental studies of the copper activation mechanisms for selective flotation of the sulfide minerals, sphalerite and pyrite.* Adv. Colloid. Interfac., 145, 97-110.

CHEN, X., SEAMAN, D., PENG, Y., BRADSHAW, D., 2014. *Importance of oxidation during regrinding of rougher flotation concentrates with a high content of sulfides*. Miner. Eng., 66, 165-172.

CRUZ, R., LUNA-Sanchez, R.M., LAPIDUS, G.T., GONZALEZ, I., MONROY, M., 2005. *An experimental strategy to determine galvanic interactions affecting the reactivity of sulfide mineral concentrates*. Hydrometallurgy, 78, 198-208.

EJTEMAEI, M., NGUYEN, A.V., 2017. *A comparative study of the attachment of air bubbles onto sphalerite and pyrite surfaces activated by copper sulphate*. Miner. Eng., 109, 14-20.

EJTEMAEI, M., PLACKOWSKI, C., Nguyen, A.V., 2016. *The effect of calcium, magnesium, and sulphate ions on the surface properties of copper activated sphalerite*. Miner. Eng., 89, 42-51.

EKMEKÇI, Z., DEMIREL, H., 1997. *Effects of galvanic interaction on collectorless flotation behaviour of chalcopyrite and pyrite*. Int. J. Miner. Process., 52, 31-48.

ESTRADA-DE Los Santos, F., RIVERA-SANTILLAN, R.E., TALAVERA-ORTEGA, M., BAUTISTA, F., 2016. *Catalytic and galvanic effects of pyrite on ferric leaching of sphalerite*. Hydrometallurgy, 163, 167-175.

FENG, Q., Wen, S., DENG, J., ZHAO, W., 2017. *DFT study on the interaction between hydrogen sulfide ions and cerussite (110) surface*. Appl. Surf. Sci., 396, 920-925.

FINCH, J.A., RAO, S.R., 1988. *Galvanic interaction studies on sulphide minerals*. Can. Metall. Quart., 27, 253-259.

FORNASIERO, D., LI, F., RALSTON, J., SMART, R.S.C., 1994. *Oxidation of Galena Surfaces: I. X-Ray Photoelectron Spectroscopic and Dissolution Kinetics Studies*. J. Colloid. Interf. Sci., 164, 333-344.

GAO, Y., GAO, Z., SUN W., HU, Y., 2016. *Selective flotation of scheelite from calcite: A novel reagent scheme*. Int. J. Miner. Process., 154, 10-15.

GAO, Z., LI, C., SUN, W., HU, Y., 2017. *Anisotropic surface properties of calcite: A consideration of surface broken bonds*. Colloids Surf. A, 520, 53-61.

GAO, Z., SUN, W., HU, Y., 2014. *Mineral cleavage nature and surface energy: Anisotropic surface broken bonds consideration*. Trans. Nonferrous Met. Soc. China, 24(9), 2930-2937.

GERSON, A.R., LANGE, A.G., PRINCE, K.E., SMART, R.S., 1999. *The mechanism of copper activation of sphalerite*. Appl. Surf. Sci., 137, 207-223.

HARMER, S.L., MIERCZYNSKA-VASILEV, A., BEATTIE, D.A., SHAPTER, J.G., 2008. *The effect of bulk iron concentration and heterogeneities on the copper activation of sphalerite*. Miner. Eng., 21, 1005-1012.

HU, Y., GAO, Z., SUN, W., LIU X., 2012. *Anisotropic surface energies and adsorption behaviors of scheelite crystal*. Colloids Surf. A, 415(1), 439-448.

NOOSHABADI, J.A, RAO, H. K., 2014. *Formation of hydrogen peroxide by galena and its influence on flotation*. Adv. Powder Technol., 25, 832-839.

JIAO, F., WU, J., QIN, W., WANG, X., LIU, R., 2016. *Interactions of tert dodecyl mercaptan with sphalerite and effects on its flotation behavior*. Colloids Surf. A, 506, 104-113.

KE, B., LI, Y., CHEN, J., ZHAO, C., CHEN, Y., 2016. *DFT study on the galvanic interaction between pyrite (100) and galena (100) surfaces*. Appl. Surf. Sci., 367, 270-276.

LEIRO, J.A., TORHOLA, M., LAAJALEHTO, K., 2017. *The AFM method in studies of muscovite mica and galena surfaces*. J. Phys. Chem. Solids., 100, 40-44.

LIU, J., WEN, S., CHEN, X., BAI, S., LIU, D., 2013. *DFT computation of Cu adsorption on the S atoms of sphalerite (110) surface*. Miner. Eng., 46, 1-5.

LONG, X., CHEN, J., CHEN, Y., 2016. *Adsorption of ethyl xanthate on ZnS(110) surface in the presence of water molecules: A DFT study*. Appl. Surf. Sci., 370, 11-18.

MARTIN, C.J., RAO, S.R., FINCH, J.A., LEROUX, M., 1989. *Complex sulphide ore processing with pyrite flotation by nitrogen*. Inter. J. Miner. Process., 26, 95-110.

MIKHLIN, Y., KARACHAROV, A., TOMASHEVICH, Y., SHCHUKAREV, A., 2016. *Interaction of sphalerite with potassium n-butyl xanthate and copper sulfate solutions studied by XPS of fast-frozen samples and zeta-potential measurement*. Vacuum, 125, 98-105.

MIKHLIN, Y., VOROBYEV, S., ROMANCHENKO, A., 2016. *Ultrafine particles derived from mineral processing: A case study of the Pb-Zn sulfide ore with emphasis on lead-bearing colloids*. Chemosphere, 147, 60-66.

MU, Y., LI, L., PENG, Y., 2017. *Surface properties of fractured and polished pyrite in relation to flotation*. Miner. Eng., 101, 10-19.

MU, Y., PENG, Y., LAUTEN, R.A., 2016. *The depression of pyrite in selective flotation by different reagent systems – A Literature review*. Miner. Eng., 96, 143-156.

OWUSU, C., BRITO e Abreu, S., SKINNER, W., ADDAI-MENSAH, J., ZANIN, M., 2014. *The influence of pyrite content on the flotation of chalcopyrite/pyrite mixtures*. Miner. Eng., 55, 87-95.

OWUSU, C., FORNASIERO, D., ADDAI-MENSAH, J., ZANIN, M., 2015. *Influence of pulp aeration on the flotation of chalcopyrite with xanthate in chalcopyrite/pyrite mixtures*. Inte. J. Miner.Process., 134, 50-57.

QIN, W., WANG, X., MA, L., JIAO, F., 2015. *Electrochemical characteristics and collectorless flotation behavior of galena: With and without the presence of pyrite*. Miner. Eng., 74, 99-104.

LIU, Q.Y., LI, H.P., LI, Z., 2007. *The Study on the Galvanic Effect of Sulphide Minerals: A Review*. Bulletin of Mineralogy Petrology and Geochemistry, 26, 284-289 (in Chinese).

SANTOS, F.E., RIVERA-SANTILLAN, R.E., TALAVERA-ORTEGA, M., BAUTISTA, F., 2016. *Catalytic and galvanic effects of pyrite on ferric leaching of sphalerite*. Hydrometallurgy, 163, 167-175.

SONG, S.X., LOPEZ-VALDIVIESO, A., REYES-BAHENA, J.L., BERMEJO-PEREZ, H.I., 2001. *Hydrophobic flocculation of sphalerite fines in aqueous suspensions induced by ethyl and amyl xanthates*. Colloids Surf. A, 181, 159-169.

TRAHAR, W.J., SENIOR, G.D., SHANNON, L.K., 1994. *Interactions between sulphide minerals — the collectorless flotation of pyrite*. Inter. J. Miner. Process., 40, 287-321.

URBANO, G., MELENDEZ, A.M., REYES, V.E., VELOZ, M.A., GONZALEZ, I., 2007. *Galvanic interactions between galena-sphalerite and their reactivity*. Inter. J. Miner. Process., 82, 148-155.

WANG J., GAO, Z., GAO, Y., HU, Y., SUN, W., 2016. *Flotation separation of scheelite from calcite using mixed cationic/anionic collectors*. Miner. Eng., 98, 261-263.

RAO, M.K., NATARAJAN, K.A., 1989. *Electrochemical effects of mineral-mineral interactions on the flotation of chalcopyrite and sphalerite*. Inter. J. Miner. Process., 27, 279-293.

ZHANG, Q., XU, Z., BOZKURT, V., FINCH, J.A., 1997. *Pyrite flotation in the presence of metal ions and sphalerite*. Inter. J. Miner. Process., 52, 187-201.